Elsevier Editorial System(tm) for Icarus
Manuscript Draft

Manuscript Number:

Title: Sodium Atoms in the Lunar Exotail: Observed Velocity and Spatial Distributions

Article Type: Regular Article

Keywords: Aeronomy; Moon; Satellites, atmospheres; Solar wind

Corresponding Author: Graduate Student Michael Line,

Corresponding Author's Institution: California Institute of Technology

First Author: Michael R Line

Order of Authors: Michael R Line; Edwin J Mierkiewicz; Ronald J Oliversen; Jody K Wilson; Matt Haffner

Abstract: The lunar sodium tail extends long distances due to radiation pressure on sodium atoms in the lunar exosphere. Our earlier observations determined the average radial velocity of sodium atoms moving down the lunar tail beyond Earth along the Sun-Moon-Earth line (i.e., the anti-lunar point) to be 12.4 km/s. Here we use the Wisconsin H-alpha Mapper to obtain the first kinematically resolved maps of the intensity and velocity distribution of this emission over a $15 \times 15 \deg$ region on the sky near the anti-lunar point. We present both spatially and spectrally resolved observations obtained over four nights around new moon in October 2007. The spatial distribution of the sodium atoms is elongated along the ecliptic with the location of the peak intensity drifting 3 degrees east along the ecliptic per night. Preliminary modeling results suggest that the spatial and velocity distributions in the sodium exotail are sensitive to the near surface lunar sodium velocity distribution and that observations of this sort along with detailed modeling offer new opportunities to describe the time history of lunar surface sputtering over several days.

Suggested Reviewers: Michael Mendillo
mendillo@bu.edu

Andrew Potter
apotter@noao.edu

Allen Stern
alan@boulder.swri.edu

Opposed Reviewers:

Highlights

Lunar exospheric sodium atoms escape from the moon and accelerate in the anti-solar direction due to solar radiation pressure forming a comet-like sodium tail> We measure the intensity and velocity distribution of the lunar sodium tail > Data/model comparisons indicate that sodium tail intensity and velocity distribution is sensitive to the near surface velocity distribution, abundance and photoionization lifetime > Measurements of the lunar sodium tail can help constrain lunar exospheric source mechanisms

DRAFT VERSION SEPTEMBER 24, 2011
Preprint typeset using LaTeX style emulateapj v. 08/13/06

SODIUM ATOMS IN THE LUNAR EXOTAIL: OBSERVED VELOCITY AND SPATIAL DISTRIBUTIONS

MICHAEL R. LINE
Division of Geological and Planetary Sciences, California Institute of Technology, Pasadena, CA 91106

E.J. MIERKIEWICZ
Department of Physics, University of Wisconsin, Madison, WI, USA.

R.J. OLIVERSEN
NASA Goddard Space Flight Center,Greenbelt, MD, USA

J.K. WILSON
Space Science Center, University of New Hampshire, Durham, NH, USA.

L.M. HAFFNER
Department of Astronomy, University of Wisconsin, Madison, WI, USA.

F.L. ROESLER
Department of Physics, University of Wisconsin, Madison, WI, USA.
Draft version September 24, 2011

ABSTRACT

The lunar sodium tail extends long distances due to radiation pressure on sodium atoms in the lunar exosphere. Our earlier observations determined the average radial velocity of sodium atoms moving down the lunar tail beyond Earth along the Sun-Moon-Earth line (i.e., the anti-lunar point) to be 12.4 km/s. Here we use the Wisconsin H-alpha Mapper to obtain the first kinematically resolved maps of the intensity and velocity distribution of this emission over a 15×15 deg region on the sky near the anti-lunar point. We present both spatially and spectrally resolved observations obtained over four nights around new moon in October 2007. The spatial distribution of the sodium atoms is elongated along the ecliptic with the location of the peak intensity drifting 3 degrees east along the ecliptic per night. Preliminary modeling results suggest that the spatial and velocity distributions in the sodium exotail are sensitive to the near surface lunar sodium velocity distribution and that observations of this sort along with detailed modeling offer new opportunities to describe the time history of lunar surface sputtering over several days.

Subject headings:

1. INTRODUCTION

The Moon is known to have a trace atmosphere of helium (He), argon (Ar), sodium (Na), potassium (K) and other trace species [see e.g., *Stern* 1999]; however its tenuous nature makes remote observations of elements other than the alkalis difficult. Sodium "D-line" emission at 5895.924 Å (D1) and 5889.950 Å (D2) has been used since the late 1980s to observe the morphology and dynamics of the lunar sodium atmosphere beginning with its detection by *Potter and Morgan* [1988] and *Tyler et al.* [1988]. Likely source mechanisms are: thermal desorption, photo-desorption, ion sputtering and meteoric impact ablation. The relative importance of these mechanisms remains uncertain, both with regard to spatial and to temporal trends. Once released, sputtered gases in the lunar atmosphere can be pulled back to the regolith by gravity, escape to space, get pushed away by solar radiation pressure, or become photoionized and swept away by the solar wind.

Electronic address: mrl@gps.caltech.edu
[1] Correspondence to be directed to mrl@gps.caltech.edu

Mendillo et al. [1991] obtained the first broadband imaging observations (D1 + D2) of the extended lunar sodium atmosphere, observing emission out to ~5 lunar radii (R_m) on the dayside, and out to 15–20 R_m in a "tail-like" structure on the nightside. The lunar sodium tail is now known to extend to great distances (many hundreds, and perhaps thousands, of lunar radii) due to the strong influence of the Sun's radiation pressure on Na atoms in the lunar exosphere [*Wilson et al.*, 1999]. Near new Moon phase, the extended lunar sodium tail can be observed as it sweeps over the Earth and is gravitationally-focused into a visible sodium "spot" in the anti-solar direction [*Smith et al.*, 1999; *Matta et al.*, 2009]. Refer to Figure 1.

Velocity resolved observations of the extended lunar sodium tail (observed in the anti-lunar direction) were first obtained by *Mierkiewicz et al.* [2006a] using a large aperture (15 cm) double etalon Fabry-Perot spectrometer with ~ 3.5 km/s spectral resolution at 5890 Å; see *Mierkiewicz et al.* [2006b] for further instrument details. Observations were made within 2–14 hours of new Moon

from the Pine Bluff Observatory (PBO), Wisconsin, on 29 March 2006, 27 April 2006 and 28 April 2006. The average observed radial velocity of the lunar sodium tail in the vicinity of the anti-solar/lunar point for the three nights was 12.4 km/s (from geocentric zero). This velocity is consistent with sodium atoms escaping from the Moon and being accelerated by radiation pressure for 2+ days. In some cases the line profile appeared asymmetric, with lunar sodium emission well in excess of 12.4 km/s.

In this paper we report new results using the unique mapping capabilities of the Wisconsin H-alpha Mapper (WHAM), where we have traded spectral resolution in favor of increased sensitivity and spatial resolution.

2. INSTRUMENTATION

WHAM was built to map the distribution and kinematics of ionized gas in our Galaxy [*Haffner et al.*, 2003]. Here we leverage WHAM's unique combination of high sensitivity, spectral resolution and automated pointing capabilities to map Na emission in the extended lunar sodium tail. At the time of these observations WHAM was located at Kitt Peak Observatory, AZ.

Similar in design to the PBO Fabry-Perot used in our earlier work, WHAM is a large aperture (15 cm) double etalon Fabry-Perot coupled to a siderostat with a circular 1 deg field-of-view (FOV). WHAM has a resolving power of 25,000, covering a 200 km/s spectral region with 12 km/s spectral resolution at 5890 Å [*Haffner et al.*, 2003].

3. OBSERVATIONS & REDUCTION

Using WHAM we have mapped the intensity and velocity distribution of the extended lunar sodium tail over a 15×15 deg region near the anti-lunar point with 1 deg spatial resolution. Observations were made during 4 nights bracketing the 11 October 2007 (5:01 UT) new moon period. The automated pointing capability of WHAM was used to build a map of the lunar Na emission by rastering WHAM's 1 deg circular FOV in a "block" surrounding the anti-lunar point. The number of 1 deg pointings per block was between 121 and 256. The exposure time for each observation was 120 s; a map was generated in approximately 6 hours. These observations provide the first kinematically resolved maps of the extended lunar sodium tail observed in the anti-lunar direction.

Individual WHAM spectra were reduced with a 4 component model: one Gaussian component for an atmospheric OH feature near -90 km/s from geocentric zero, a second Gaussian component for an unidentified feature near -70 km/s, a Voigt profile for the terrestrial sodium emission at 0 km/s and a Gaussian component for the lunar emission near 13 km/s; Refer to Figure 2a.

Due to the partial blending of the terrestrial and lunar Na emission, the component fitting of the WHAM data required two steps. First, a constrained fit was applied to the data in which the Doppler shift of the lunar emission with respect to the terrestrial sodium sky glow line was fixed at 12.5 km/s based on our experience with the higher resolution PBO observations. Next, after a best-fit solution was obtained, the Doppler separation of the lunar emission was freed and the fitting routine was run again. In all cases, fit components were convolved with an instrumental profile and iterated, subject to the above constraints, to produce a least squares, best-fit to the data using the Voigt-fit code of *Woodward* [2011].

After fitting we plot the lunar sodium emission spectra as a function of position on the sky (Figure 2b). The intensity (i.e., the integrated area under the emission line, converted to Rayleighs, where 1R = $10^6/4\pi$ photons cm^{-2} s^{-1} str^{-1}) of the lunar sodium emission is then converted into colored beams representing WHAM's 1 deg field-of-view on the sky (Figure 2c). These beams are then smoothed (Figure 2d). We also generate a spatial map for the Doppler widths (full-width-at-half-maximum) of the lunar sodium emission lines.

Intensity calibration is based on the surface brightness of NGC 7000, the "North American Nebula" (coordinates α_{2000} = 20.97 h, δ_{2000} = 44.59 deg). The NGC 7000 hydrogen Balmer α (6563 Å) surface brightness is $\sim$ 800 R over WHAM's 1 deg field-of-view [*Haffner et al.*, 2003]. Sodium D2 line intensities are based on the assumption that WHAM's efficiency is unchanged between 6565 Å and Na, and a measured filter transmission ratio of T(5890 Å)/ T(6563 Å) $\sim$ 1. We estimate a 20% uncertainty in our sodium D2 intensity calibration.

4. RESULTS

Spectra for the brightest beam for each night are given in Figure 3 and Table 1. Intensity and Doppler width maps for all pointings are given in Figure 4.

In look directions where the lunar Na emission is below our detection limit, a small amount of emission will nonetheless be attributed to lunar Na emission in our Gaussian component fitting procedure. In order to determine this detection threshold, we mapped a region of the sky 60 deg east of the anti-lunar point. This off-direction dataset was processed with the Gaussian fitting procedure used in the analysis of the on-direction datasets (as described in Section 3) in order to assess the amount of emission attributed to lunar Na emission when none is present. We found the average intensity of the background emission to be 0.7 R; intensities lower than this value should not be mistaken as an indication of lunar Na emission in the maps presented in Figure 4.

In what follows we present a basic description of the observations for each night.

10 October 2007: Observations 22 to 16 hours before new moon (first column of Figure 4), 169 1 deg pointings. The intensity distribution is elongated along the ecliptic with the location of the peak intensity to the south-west of the antisolar point. The Doppler width distribution appears to peak to the north-east of the brightest emission and is also elongated along the ecliptic. The broadest emission is also the faintest emission for this night. The brightest emission occurs approximately 10.8 deg from the antisolar point, southeast along the ecliptic, with a peak intensity of 2.2 R.

11 October 2007: Observations 1 hour before to 7 hours after new moon (second column of Figure 4), 224 1 deg pointings. The intensity distribution is nearly axially symmetric; the Sun, Moon and Earth are aligned, meaning we are looking almost directly down the lunar tail. As with the previous night, the peak intensity is to the south-west of the antisolar point. The broadest emission for this night is also the brightest emission. The peak emission occurs 5.8 deg southeast of

the anti-solar point, coplanar not necessarily colinear.

12 October 2007: Observations 23 to 32 hours after new moon (third column of Figure 4), 256 1 deg pointings. The intensity distribution again appears to be elongated along the ecliptic with the brightest emission occurring closer to the antisolar point and the fainter emission occurring farther to the south-east. From the Doppler width map it appears that there is a large region where the widths are roughly 15-20 km/s, with the broadest emission falling roughly in the same location as the brightest emission 2.7 deg from the antisolar point.

13 October 2007: Observations 48 to 52 hours after new moon (fourth column of Figure 4), 121 1 deg pointings. The emission is extremely faint and remains elongated along the ecliptic. The broadest emission, upwards of 30 km/s, for this night appears to peak to the southwest of the brightest emission. The brightest emission is 1.8 deg to the southeast of the antisolar point.

5. SAMPLE MODEL RUNS

We present a sample set of data/model comparisons using the numerical/Monte-Carlo lunar exospheric simulation code of *Wilson et al.* [1999; 2003] to indicate the potential of future model/data analysis.

The *Wilson et al.* [1999; 2003] code uses 4th order Runga-Kutta integration to compute the accelerations and positions of exospheric sodium atoms due to gravitational and solar radiation pressure effects. Model input parameters include the atom's initial velocity distribution and their surface ejection rate, ionization lifetime and initial source distribution (e.g., isotropic, where atoms are evenly ejected over the entire surface of the moon, or hemispheric, where ejection is favored on the sunlit side of the moon).

Because our maps were constructed over roughly a six hour interval per night, data/model comparisons were done using an average spectrum over the full map area in order to circumvent spatial smearing between the observations conducted over a span of hours and the model distribution computed for fixed time. All model runs assumed that the lunar sodium source was distributed isotropically over the Moon's surface. Both the data and model averages were normalized for these comparisons. Model calculations were made with 1 deg spatial resolution to match the 1 deg spatial resolution of the WHAM spectrometer. Model spectra are generated with significantly higher velocity resolution than WHAM's spectral resolution of 12 km/s. As such, model output was convolved with a WHAM instrumental function in order to facilitate direct data/model comparisons. In order to eliminate sodium photoionization lifetime effects from our model generated line profiles, a Na photoionization lifetime of 100 hrs was used for this sample study.

In Figure 5 we investigate how variations in the initial sodium particle velocity distribution at the Moon manifest themselves in our observed line profile observations of the extended Na tail (11 October 2007 dataset). The solid line in Figure 5 is an average line profile for all WHAM observations obtained on 11 October 2007, normalized to the peak intensity; the dashed line is the corresponding model run average normalized to its peak intensity.

Three different initial velocity distributions were used in our data/model comparison: slow (initial velocities falling between 2.1 and 2.15 km/s), fast (initial velocities falling between 2.56 and 2.6 km/s) and flat (i.e., and equal number of particles leaving the moon with velocities of 2.1 – 2.6 km/s). These velocity distributions are based on the work of *Wilson et al.* [1999; 2003]; although the initial velocity distribution was not fully constrained by *Wilson et al.* [1999; 2003], the 2003 paper did show that there is a significant contribution to the extended lunar Na tail from source speeds in the range of 2.1–2.4 km/s, thus the choice of 2.1– 2.6 km/s velocity range used in this study.

Inspection of Figure 5 indicates that the shape of the observed and modeled line profiles in the anti-lunar direction near the time of new moon are sensitive to the initial velocity distribution of the sodium atoms leaving the moon. A fast initial velocity distribution results in a much broader average spectrum whereas a slow initial distribution produces a much narrower spectrum. It is important to emphasize that changes in the lunar source rates $\sim$ 2 days prior to the observations (when the observed Na atoms were being released from the lunar surface) could produce similar signatures, as would changes in the sodium photoionization lifetime due to solar activity. The flat velocity distribution produces a spectrum closest to that observed, see Figure 5, lower right.

Figure 6 shows model runs for the other three nights of observations (plus 11 October 2007), using the flat initial velocity distribution. In this case model spectra were computed and averaged over the observation time ranges for each night (refer to Section 4). The spatial averaging is handled in the same manner as Figure 5.

Although the data/model high velocity tail trends shown in Figure 6 qualitatively agree for each night, given our use of a 100 hr sodium atom photoionization lifetime in the model runs presented here, too many atoms are surviving to high velocity. This effect is especially apparent in Figure 6, bottom right (13 October 2007), where the model emission (dotted line) is significantly enhanced relative to the observations. Future runs using a sodium photoionization lifetime closer to the currently accepted value of 45 hours at 1 A.U. from the Sun [*Huebner*, 1992] are expected to reduce the number of neutral sodium atoms surviving to high velocity.

6. CONCLUSIONS

Over the course of 4 nights ($\sim$70 hours) of observations, the peak of the intensity distribution (see Figure 4 and Table 1) drifted east along the ecliptic a total $\sim$ 11.5 deg (an average of 0.2 deg per hour), consistent with the 3–4 deg eastward drift per day observed by *Smith et al.* [1999]. For reference, the lunar orbital rate is about 0.5 deg per hour. The brightest detected emission occurred on the night of new moon, presumably because the observation geometry at new moon presents the most direct look down the lunar tail (and hence the maximum column emission).

The broadest emission was detected on the nights away from new moon, occurring north-east of the peak intensity for the night preceding new moon, and to the south-west following new moon. It would appear that this observed change in morphology is related to viewing geometry.

At new Moon the nearby bright "core" of Na atoms recently gravitationally focused by the Earth [*Wilson et al.*, 1999] dominates the tails appearance, giving it a nearly axisymmetric core emission at 12.5 km/s, obscuring the dimmer signal of the older (and faster) more distant atoms; refer to Figure 4 column 2. Before and after new Moon, however, the Earth's gravity only influences atoms at one outer edge of the sodium tail and the tail is observed off-axis, leaving relatively more atoms in an extended diffuse "un-focused" tail away from the 12.5 km/s core emission and a correspondingly larger influence on the Doppler width observed in our data.

Our sample model runs and recent work by *Lee et al.* [2011] confirm that velocity resolved observations and spatial mapping of the extended lunar tail offer new opportunities to describe the time history of lunar surface sputtering over several days, and set constraints for models of exospheric source mechanisms and their variabilities.

The authors thank M. Mendillo and R. Reynolds for their valuable assistance. We thank all the members of the WHAM collaboration, in particular K. Jaehnig, A. Hill, G. Madsen and K. Barger. Finally, we thank the National Solar Observatory mountain support staff, C. Plymate and E. Galayda for their support and hosting us during the WHAM observations. M. Line's involvement as an undergraduate at Wisconsin was partially supported by a UW-Madison Hilldale Undergraduate Fellowship. This work has also been partially funded by NASA award NNX11AE38G.

REFERENCES

Haffner, L. M., R. J. Reynolds, S. L. Tufte, G. J. Madsen, K. P. Jaehnig, and J. W. Percival (2003), The Wisconsin Hα Mapper Northern Sky Survey, *The Astrophysical Journal Supplement Series*, *149* (2), 405-422, doi:10.1086/378850.

Huebner, W. F., J. J. Keady, and S. P. Lyon (1992), Solar photo rates for planetary atmospheres and atmospheric pollutants, *Astrophysics and Space Science*, *195*, 1-289, doi:10.1007/BF00644558.

Lee, Dong-Wook, S. J. Kim, D. Lee, H. Jin, K. Kim (2011), Three-dimensional simulations of the lunar sodium exosphere and its tail, *Journal of Geophysical Research*, *116*, A7, doi:10.1029/2011JA016451

Matta, M., S. Smith, J. Baumgardner, J. Wilson, C. Martinis, M. Mendillo (2009), The sodium tail of the Moon, *Icarus*, *204* (2), 409-417, doi:10.1016/j.icarus.2009.06.017.

Mendillo, M., J. Baumgardner, B. Flynn (1991), Imaging observations of the extended sodium atmosphere of the moon, *Geophysical Research Letters*, *18* 2097-2100, doi:10.1029/91GL02622.

Mierkiewicz, E. J., M. Line, F. L. Roesler, R. J. Oliversen (2006a), Radial velocity observations of the extended lunar sodium tail, *Geophysical Research Letters*, *33*, (20), doi:10.1029/2006GL027650.

Mierkiewicz, E. J., F. L. Roesler, S. M. Nossal, and R. J. Reynolds (2006b), Geocoronal hydrogen studies using Fabry Perot interferometers, part 1: Instrumentation, observations, and analysis, *Journal of Atmospheric and Solar-Terrestrial Physics*, *68* (13), 1520-1552, doi:10.1016/j.jastp.2005.08.024.

Potter, A. E., T. H. Morgan (1988), Discovery of sodium and potassium vapor in the atmosphere of the moon *Science*, *241*, 675-680, doi:10.1126/science.241.4866.675.

Smith, S. M., J. K. Wilson, J. Baumgardner, M. Mendillo (1999), Discovery of the distant lunar sodium tail and its enhancement following the Leonid meteor shower of 1998 *Geophysical Research Letters*, *26*, (12), 1649-1652, doi:10.1029/1999GL900314.

Stern, S. A. (1999), The lunar atmosphere: History, status, current problems, and context *Reviews of Geophysics*, *37*, (4), 453-492, doi:10.1029/1999RG900005.

Tyler, A. L., D. M. Hunten, R. Kozlowski (1988), Observations of sodium in the tenuous lunar atmosphere *Geophysical Research Letters*, *15*, 1141-1144, doi:10.1029/GL015i010p01141.

Wilson, J. K., S. M. Smith, J. Baumgardner, M. Mendillo (1999), Modeling an enhancement of the lunar sodium tail during the Leonid meteor shower of 1998 *Geophysical Research Letters*, *26*, (12), 1645-1648, doi:10.1029/1999GL900313.

Wilson, J. K., J. Baumgardner, M. Mendillo (2003), The outer limits of the lunar sodium exosphere, *Geophysical Research Letters*, *30*, (12), 51-1, doi:10.1029/2003GL017443.

Woodward. R. C. (2011), A parameter estimation technique for spectral analysis of overlapping lines, *JQSRT*, submitted 9/2011.

TABLE 1
October 2007 WHAM extended lunar sodium tail observations. The right ascension (α), declination (δ), Intensity, Doppler Shift and Doppler Width (fwhm) are given for the brightest pointing for each night. The new moon occurred on 11 October at 5:01 UTC.

Obs. Time/Date (UTC)	α (hh:mm)	δ (deg)	Intensity (R)	Doppler Shift (km/s)	Doppler Width (km/s)
08:30 10 Oct. 2011	00:21	1.83	2.2	9.37	7.19
05:51 11 Oct. 2011	00:44	3.96	6.3	11.96	11.29
08:02 12 Oct. 2011	00:56	5.96	8.7	17.97	27.78
06:48 13 Oct. 2011	01:03	6.96	3.5	30.39	40.36

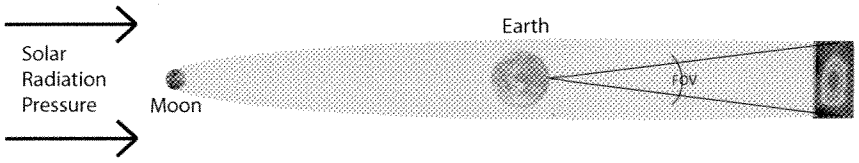

FIG. 1.— A cartoon depicting the geometry of the extended lunar sodium tail. Sodium observations are made in the anti-lunar direction near New Moon, looking down the lunar tail as it moves beyond the Earth, along the Sun-Moon-Earth line (after *Wilson et al.* [1999])

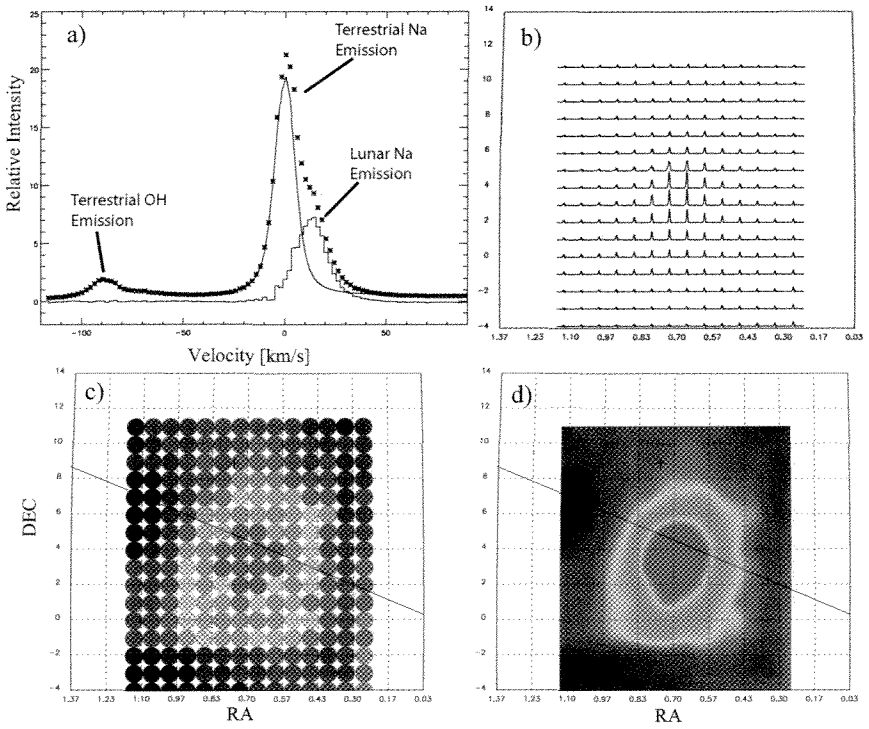

FIG. 2.— Data reduction procedure. (a) A typical spectrum showing both terrestrial (0 km/s) and Doppler shifted lunar sodium emission near 12.5 km/s. A Gaussian component fit is used to isolate and remove the terrestrial emission and to track the relative intensity and Doppler width of the lunar emission. (b) Spatial variation of the lunar sodium emission on the sky (as a function of right ascension and declination). (c) The intensity of the lunar emission is converted into a colored beam map (each beam is 1 deg on the sky). (d) Smoothed version of (c). A similar procedure is used to visualize the spatial distribution of the Doppler width of the lunar emission.

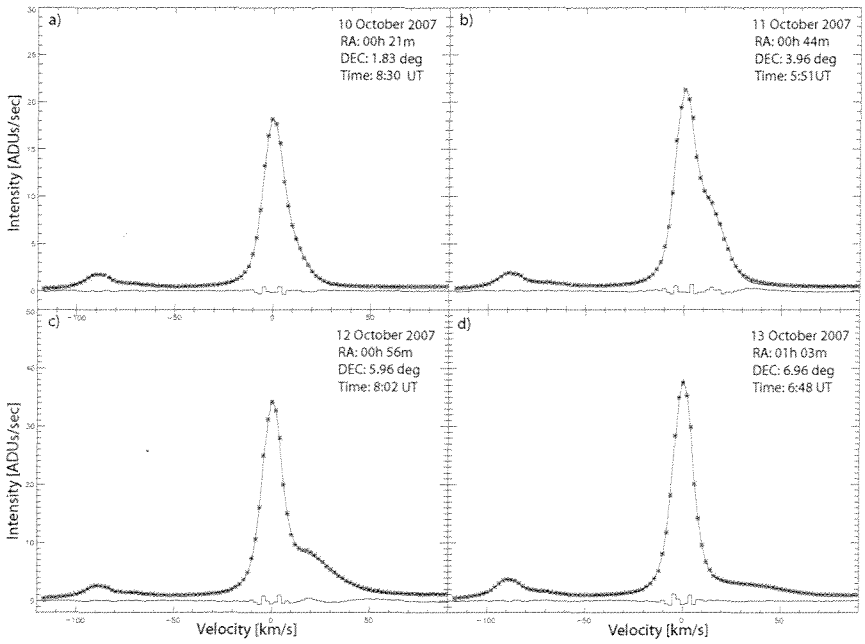

FIG. 3.— The brightest lunar emission spectra for each of the four October nights. In all cases the lunar emission is blended with the terrestrial emission; the decomposition of (b) is shown in Figure 2. The lunar emission is redward of the terrestrial emission (near 12.5 km/s). The dates, times and celestial coordinates are given in each panel.

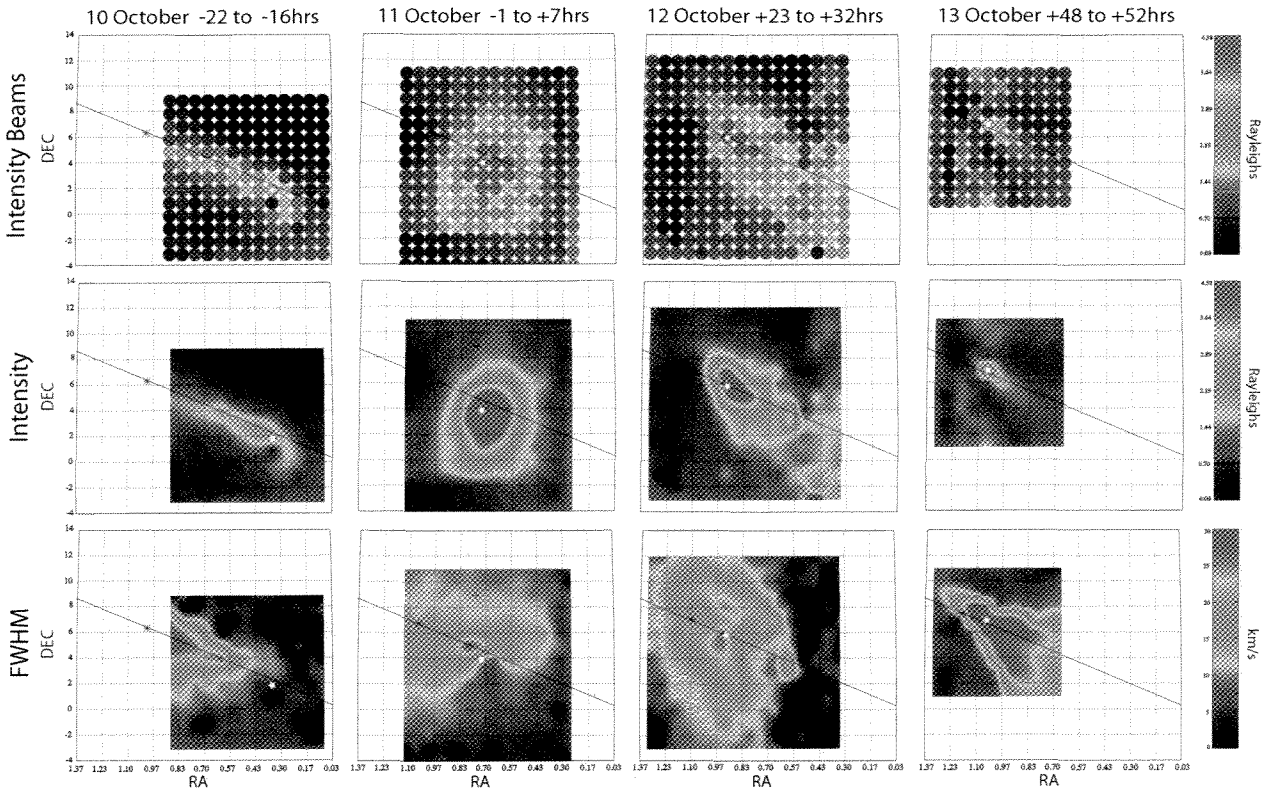

FIG. 4.— October WHAM Observations. (*top*) Regularly gridded beam maps of the lunar sodium emission for each night. The anti lunar point is indicated by the +, the anti solar point is indicated by the *. The brightest beam observed for each evening is indicated by a white star. The black line represents the ecliptic. (*middle and bottom*) Smoothed map of the spatial variation in the intensity and Doppler width (red corresponds to broader emission) of a single Gaussian fit to the lunar sodium emission. The times relative to new moon for each night are shown at the top of the Figure. The solid line on the intensity color bars denotes our confidence limit; colors/Intensities below this value are likely not due to the lunar emission (see text).

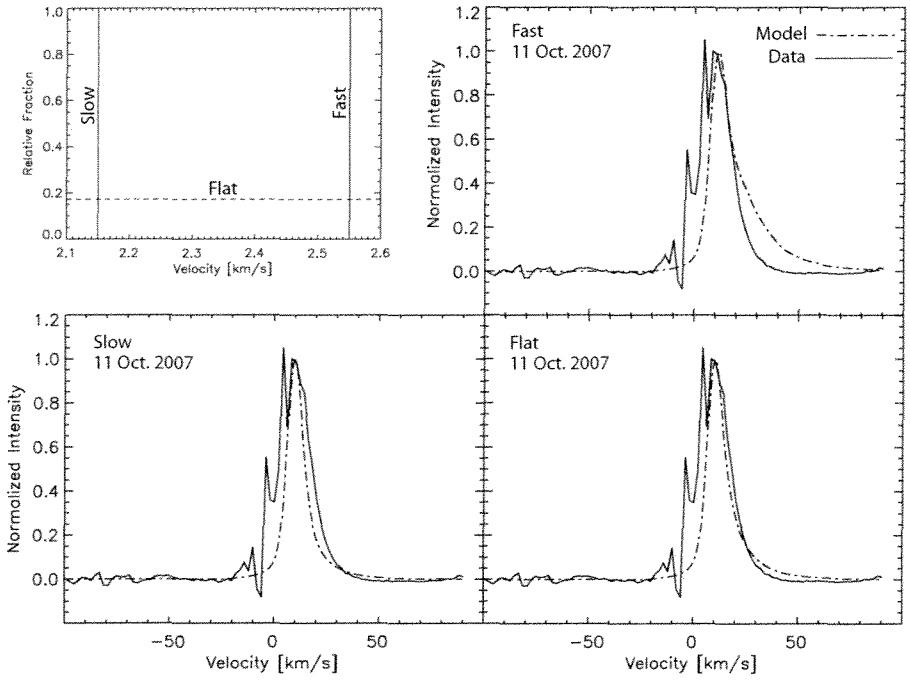

FIG. 5.— Data/model line profile comparisons using 3 different initial velocity distributions: slow, flat, fast. (*inset*) The relative fraction of the particles that fall within a particular velocity interval. The "slow" velocity distribution represents particles leaving the Moon with initial velocities that fall between 2.1–2.15 km/s. In the "fast" case, initial velocities fall between 2.56–2.6 km/s. The "flat" velocity distribution represents an initial distribution with a range of velocities between 2.1–2.6 km/s. (*top right & bottom*) Model and data comparisons using the fast, slow and flat initial velocity distributions. (The noise on the blue wing of the profile is due to the terrestrial sky glow line subtraction.)

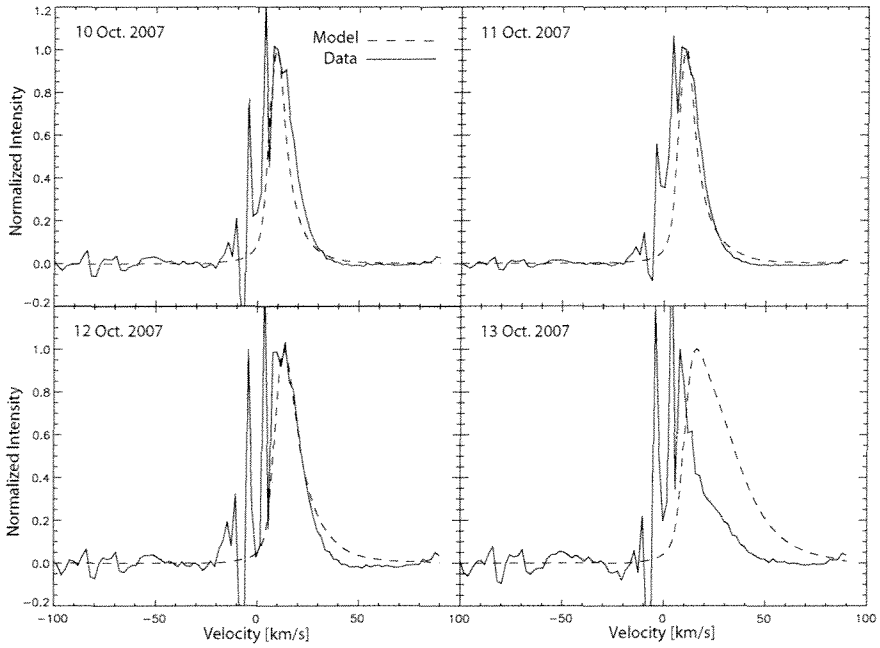

FIG. 6.— A comparison of the average spectra for each of the four October nights from WHAM and the average spectra generated for each of the October nights via the model. The solid line represents the WHAM data and the dashed line represents the spectra produced by the model. In this case model spectra were computed and averaged over the observation time ranges for each night (refer to Section 4). The spatial averaging is handled in the same manner as Figure 5. (The noise on the blue wing of the profile is due to the terrestrial sky glow line subtraction.) Excess model high velocity atom productions is likely an artifact of a too many sodium atoms surviving to high velocity given our 100 hr Na atom lifetime.